Reversible Luminescence Modulation upon an Electric Field on a Full Solid-State Device Based on Lanthanide Dimers

Xiaohui Yi,[†,‡] Jie Shang,[†,‡] Liang Pan,[†,‡] Hongwei Tan,[†,‡] Bin Chen,[†,‡] Gang Liu,[*,†,‡] Gang Huang,[§] Kevin Bernot,[*,§] Olivier Guillou,[§] and Run-Wei Li[*,†,‡]

[†]Key Laboratory of Magnetic Materials and Devices, Ningbo Institute of Materials Technology and Engineering, Chinese Academy of Sciences, Ningbo, Zhejiang 315201, P. R. China

[‡]Zhejiang Province Key Laboratory of Magnetic Materials and Application Technology, Ningbo Institute of Materials Technology and Engineering, Chinese Academy of Sciences, Ningbo, Zhejiang 315201, P. R. China

[§]Institut des Sciences Chimiques de Rennes, UMR 6226 INSA-Rennes, 20 avenue des buttes de Coësmes, 35708 Rennes, France

S *Supporting Information*

ABSTRACT: Switching luminescence of lanthanide-based molecules through an external electric field is considered as a promising approach toward novel functional molecule-based devices. Classic routes use casted films and liquid electrolyte as media for redox reactions. Such protocol, even if efficient, is relatively hard to turn into an effective solid-state device. In this work, we explicitly synthesize lanthanide-based dimers whose luminescent behavior is affected by the presence of Cu^{2+} ions. Excellent evaporability of the dimers and utilization of Cu^{2+}-based solid-state electrolyte makes it possible to reproduce solution behavior at the solid state. Reversible modulation of Cu^{2+} ions transport can be achieved by an electric field in a solid-state device, where lanthanide-related luminescence is driven by an electric field. These findings provide a proof-of-concept alternative approach for electrically driven modulation of solid-state luminescence and show promising potential for information storage media in the future.

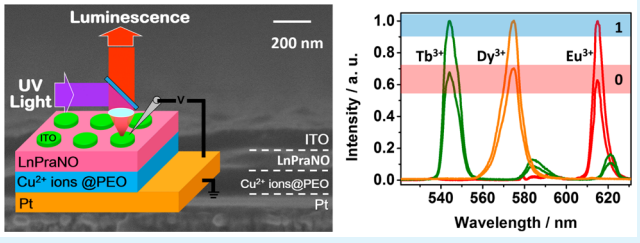

KEYWORDS: *luminescence modulation, lanthanide ions, ion transport, all-solid state, electrical driven*

INTRODUCTION

Nonvolatile manipulation of luminescence through external stimuli is considered as a fascinating and promising approach for applications such as memories, displays, and sensors.[1−5] In particular, the modulation of luminescence with an electric field as an external stimuli carries unique advantages for information storage. For instance, as the stored information can be optically and remotely read with a fast transmission rate and anti-interference characteristics,[6] a high density recording can be achieved by properly designing the structure of electronic memories.[7,8] The realization of such optoelectronic circuits requires smart luminescent molecules or materials, in which not only reversible switching of luminescence is necessary when being subjected to an external electric field but also various luminescence colors should be obtained in order to provide crosstalk-free readout among different storing units. Lanthanide-based complexes are ideal candidates for the construction of such systems because of their multicolor, narrow-bandwidth, and long-lived luminescence properties.[9] Nevertheless, the tedious film deposition procedure and the requisition of liquid supporting electrolyte for redox reactions upon the electric field still impede them from direct application.[10−12]

In this work, we propose and demonstrate a proof-of-concept strategy that combines two interesting findings for the effective modulation of luminescence of lanthanide-based complexes in the solid state: (i) the luminescence of lanthanide compounds containing Lewis basic pyridyl sites can be efficiently quenched by Cu^{2+} ions;[13,14] (ii) Cu^{2+} ions can be transported and controllably redistributed by the electrical field in solid-state media.[15−17] On the basis of the above considerations, we have synthesized a new series of lanthanide-based dinuclear complexes **LnPraNO**, of formula $[Ln(hfac)_3(PraNO)]_2$ (where Ln = Eu, Tb, and Dy, hfac = hexafluoroacetylacetonate, PraNO = pyrazine-N-oxide). These complexes are evolutions of **LnPyNO** dimers of formula $[Ln(hfac)_3(PyNO)]_2$ (PyNO = pyridine-N-oxide) that are strongly emissive and evaporable and that some of us previously reported.[18] In **LnPraNO**, the aromatic ligand that bridges the lanthanides possesses an uncoordinated Lewis basic pyridyl site that makes the luminescence of these compounds highly sensitive to the presence of Cu^{2+} ions in solution. Furthermore, ITO/**LnPraNO**/Cu^{2+} ions@PEO/Pt (ITO = indium tin oxides, PEO = poly(ethylene oxide)) structured solid-state devices based on these dimers can be designed, and we demonstrate that the reversible modulation of lanthanide-related luminescence behavior upon an electric field is possible through electric

field-induced transport of Cu^{2+} ions across the dimer-based and electrolyte layers.

RESULTS AND DISCUSSION

Single-crystals of the Dy derivative (**DyPraNO**) have been obtained, and the main structural data are reported in Table S1. Isostructurality of **EuPraNO**, **TbPraNO**, and **DyPraNO** is verified on the basis of comparison of their X-ray diffraction powder patterns (Figure S1). DyPraNO crystallizes in the *C*2/*c* space group (N°15) (Figure 1) and is similar to the previously

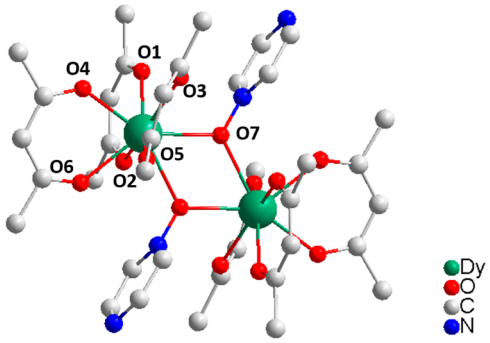

Figure 1. View of compound DyPraNO with labeling scheme. Hydrogen and fluorine atoms are omitted for clarity.

reported dimer.[18] The molecule is made of two $Dy(hfac)_3$ moieties connected by two pyrazine-N-oxide ligands. The Dy^{3+} ions are in a distorted square antiprism coordination environment close to a D4d site symmetry (Figure S2). The intramolecular Dy−Dy distance is 4.10(6) Å. Each dimer is well isolated with the shortest interdimer Dy−Dy distance of 9.12 (1) Å.

The emissive properties of all the derivatives have been investigated in the solid polycrystalline state at room temperature. As shown in Figure 2a, all compounds exhibit characteristic luminescence of lanthanide ions when excited at 350 nm. The **EuPraNO** derivatives exhibit the characteristic emission that corresponds to $^5D_0 \rightarrow {}^4F_J$ (J = 0−4) transitions. For the **TbPraNO** and **DyPraNO**, well-defined peaks are observed because of $^5D_4 \rightarrow {}^4F_J$ (J = 0−6) and $^4F_{9/2} \rightarrow {}^6H_J$ (J = 11/2−15/2) transitions, respectively. The excitation spectra of these compounds are reported in Figure S3. The quantum yields are 14.1%, 17.2%, and 0.1%, respectively.

Generally, the luminescence of lanthanide complexes is arising from the 4f electron transition from the excited states to the ground state and may be enhanced through the antenna effect. For instance, the presence of organic ligand will lead to increased absorbance of UV light, while the subsequent energy transfer from the ligands into the excited 4f state of the lanthanide ions will intensify the luminescent intensity of the material. On the other hand, the uncoordinated nitrogen atoms of the pyrazine-N-oxide ligand are expected to be good coordination sites for 3d ions such as Cu^{2+}. The interaction between the Cu^{2+} ions and the pyridyl N atoms will introduce the additional nonradiative electron exchange pathways, which may reduce the antenna efficiency of the organic ligand around lanthanide ions and quench the luminescence of the lanthanide complexes.[14] The quenching effect of Cu^{2+} has been first investigated on ethanoic solutions of the **LnPraNO** series, and a clear diminution of the luminescence intensity is observed upon addition of copper nitrate solution. Remarkably, equimolar copper-based solutions led to a 100 times reduction of the luminescence intensity on **EuPraNO** (Figure 2b). When a similar experiment is performed on the $[Eu(hfac)_3(PyNO)]_2$ dimer,[18] the compound without uncoordinated N atoms, only a 50% decrease of intensity is observed (Figure S4). This may suggest a possible Cu^{2+} coordination on the uncoordinated N atom of the pyrazine ligand. For the other derivatives of **TbPraNO** and **DyPraNO**, a decrease of 80% and 75% of the luminescence intensity is observed, respectively.

This quenching effect can be rationalized by a modified Stern−Volmer equation that describes the static and dynamic process during the quenching (1):

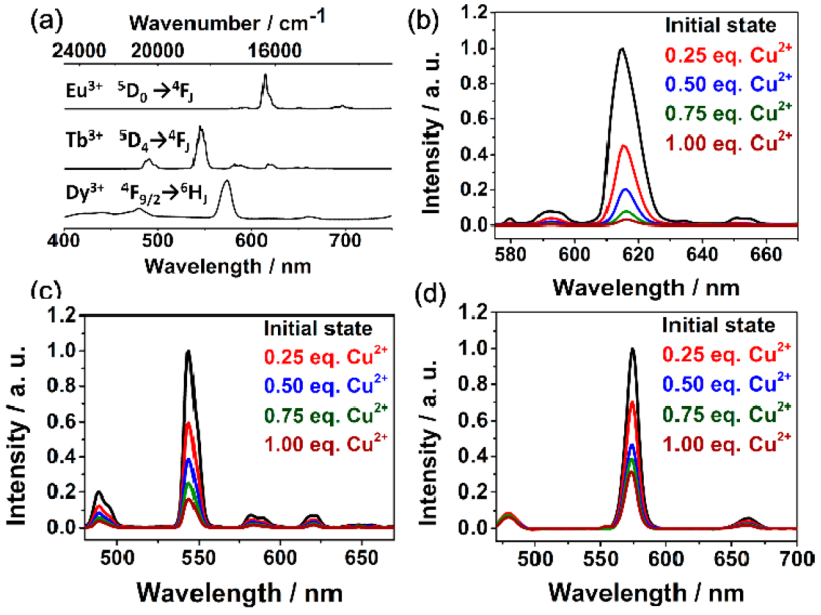

Figure 2. (a) Emission spectra of **Eu-**, **Tb-** and **DyPraNO** (from top to bottom). Evolution of the emission spectra upon addition of Cu^{2+} ions in ethanol solutions of (b) **Eu-**, (c) **Tb-**, and (d) **DyPraNO**, respectively. The excitation wavelength is set at 350 nm.

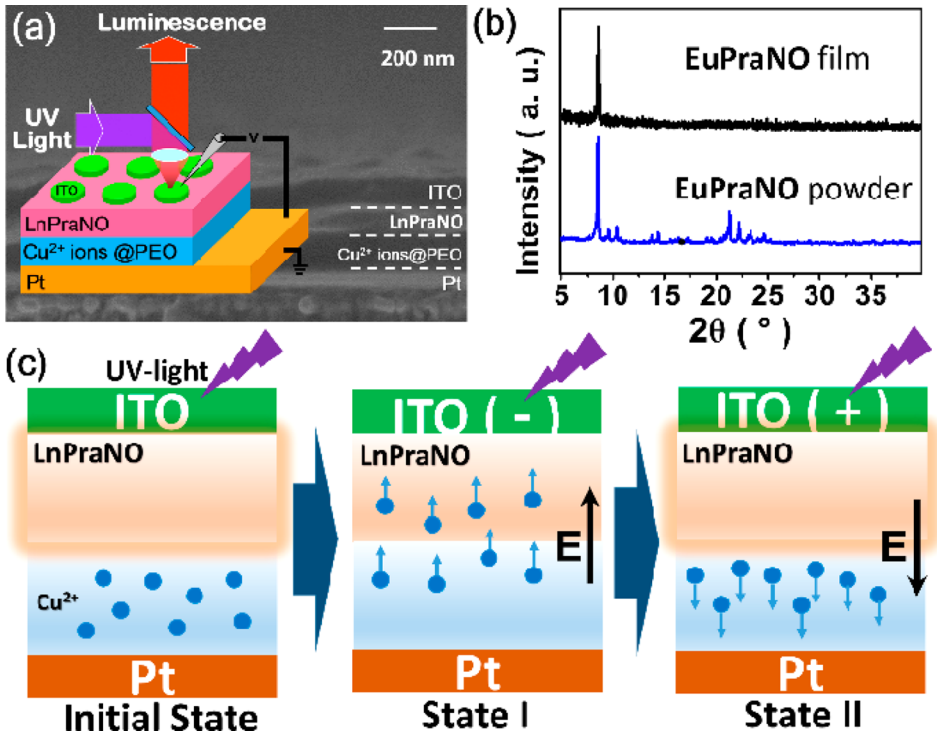

Figure 3. (a) Cross-sectional scanning electron microscopic image and schematic illustration of the ITO/**LnPraNO**/Cu^{2+}ions@PEO/Pt device. (b) X-ray diffraction pattern of the **EuPraNO** film. (c) Schematic illustration of the migration and distribution of ions upon electric field (the blue spheres stand for the mobile Cu^{2+} ions).

$$\ln(I_0/I) = \ln(1 + K_{SV}[M]) + V[M] \quad (1)$$

where I_0 and I are the luminescence intensities before and after addition of the copper nitrate solution, $[M]$ is the stochiometric ratio between the metal ion and **LnPraNO**, and K_{SV} and V are the dynamic and static quenching effect coefficients of the metal ion, respectively.[19] The V value is estimated to be 3.56, 1.78, and 1.24, for **EuPraNO**, **TbPraNO**, and **DyPraNO**, respectively, while the K_{SV} value that describes the collisional process is smaller than 0.1 (Table S2 and Figure S5).

The above findings in liquid samples provide fundamental support for the proposed target of modulating lanthanide compound luminescence in the solid state. The good volatility and robustness of **LnPraNO** make possible the design of a solid-state multilayer structure (Figures 3a,b and S6). Here, the $Cu(NO_3)_2$/PEO layer has been selected to provide the copper ions since Cu^{2+} ions containing PEO are one of the typical solid-state electrolytes.[20] ITO electrodes with good electrical conductivity and excellent optical transparency were fabricated as top electrode.[21] As illustrated in Figure 3c, when an external negative electric field is applied onto the ITO/**LnPraNO**/$Cu(NO_3)_2$@PEO/Pt device, the Cu^{2+} ions are expected to be injected into the LnPraNO layers and to provoke the quenching of the luminescence of the **LnPraNO** complexes (State I). When a positive electrical-field is applied, the Cu^{2+} ions are expected to be pumped back into the PEO hosting layer and the luminescence of **LnPraNO** complexes shall be recovered (State II).

Experimental data agreed well with the above model, and the evolution of luminescence intensity upon electric field variation for the Eu-based device is depicted in Figure 4. A negative voltage is applied for 5 s to the device in order to induce Cu^{2+} migration where the photoluminescence spectra are recorded after removing the electric field. The photoluminescence (PL) intensity changes are observed for a minimum bias voltage of −1.5 V while for −2.5 V a 60% decrease of the higher emission peak (615 nm) of **EuPraNO** is achieved (Figure 4a). When a bias voltage of 3 V is applied for 5 s and removed, the PL intensity could be recovered, suggesting that the luminescence modulation operation of the device is fully reversible and the compound was not destroyed. More importantly, the luminescent intensity remains stable when the applied electric field is switched off (e.g., after 60 s as shown in Figure 4b), indicating that nonvolatile modulation of the device luminescence has been achieved by the present strategy. By defining the highly luminescent state (Initial state and State II) as the ON state and the low luminescence state (State I) as the OFF state, repeatable ON/OFF switching behavior can be obtained in the lanthanide compound-based molecular devices (Figure 4c).

It is noteworthy that a luminescence change in these devices is not due to any redox reaction that involves the lanthanide ion. In fact, such reaction is very unlikely to occur because (i) previous studies on the electrochemical properties of lanthanide-based β-diketonate complexes demonstrate their difficult reduction in standard conditions;[22] (ii) reversibility would not be observable as a reduction may induce the decoordination of the organic ligand and the lanthanide and so annihilation of the antenna effect that promotes lanthanide luminescence in the device; (iii) solution behavior upon variable Cu^{2+} concentration (Figure 2) matches well with the observed solid-state behavior. Consequently, we can assume that the luminescent intensity change is induced by the transport and redistribution of Cu^{2+} ions by the electric field in the **LnPraNO** layer. This argument is verified by the dynamic process of the electrical field-induced PL change (Figures 4b and S7). After being stimulated with voltage pulse of −2.5 V,

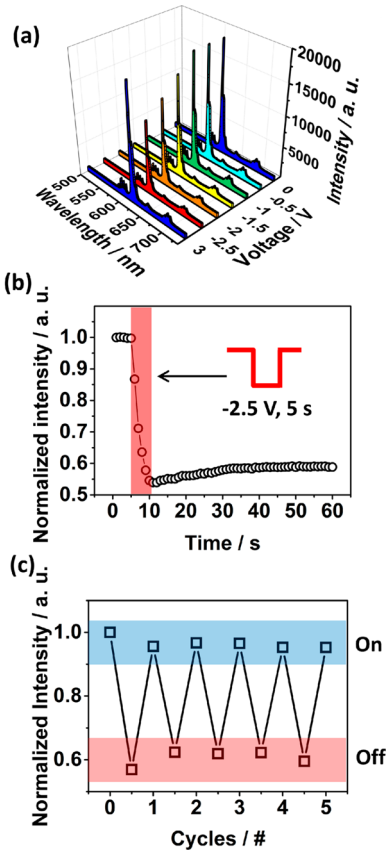

Figure 4. (a) Photoluminescence spectra of the Eu-based device after being subjected to various voltages for 5 s, respectively. (b) Time-dependent luminescence intensity of the device at 615 nm after being subjected to a voltage pulse of −2.5 V for 5 s. (c) Reproducible normalized photoluminescence intensity of the device at 615 nm against alternating negative and positive electric fields. (The luminescent intensity is normalized by the initial luminescent intensity of the device at 615 nm.)

PL intensity at 615 nm drops at 53% of its nominal value and then relaxes around 60% of the original PL intensity. This phenomenon is quite similar to the resistance relaxation induced by an ionic transport discussed in a previous work.[23] The content of the Cu^{2+} ions injected upon −2.5 V was estimated to be 0.20 molar fraction of **EuPraNO** molecules in the luminescent layer according to eq 1. This is in agreement with the behavior observed in solution.

To further confirm the efficiency of the pyrazine ligand toward Cu^{2+} coordination, a device based on the pyridine-based dimers previously mentioned (**EuPyNO**) is constructed and exposed to the very similar operating conditions.[18] It shows a lower quenching effect (80% instead of 60% of the nominal intensity is conserved; Figure S8). This may support the hypothesis of a strong interaction of the Cu^{2+} ions with the uncoordinated N atoms in the pyrazine-based emissive layer as targeted in this study.

The devices based on Tb and Dy derivatives as a luminescent layer exhibit similar but less spectacular voltage-induced luminescence modulation behaviors. For a −2.5 V voltage, the luminescent intensities of the Tb- and Dy-based devices are quenched about 65% and 70%, respectively, as shown in Figure 5a,b. The Cu^{2+} ions injected are estimated to be 0.21 and 0.26 mole fraction of the **LnPraNO** molecules in the layers according to eq 1, for Tb- and Dy-based devices, respectively. These values are once again in agreement with what is observed in solution together with the less efficient quenching effect compared with the Eu-based device. Similar to the ITO/**EuPraNO**/$Cu(NO_3)_2$@PEO/Pt unit, the photoluminescence of each measured Dy- and Tb-based unit could be recovered when a positive potential was set at 3 V for 5 s. The luminescent switching is reversible as well (Figure 5c,d). The modulation of the Eu^{3+}-, Tb^{3+}-, and Dy^{3+}-related luminescence with their distinguishable colors of red, green, and yellow, respectively, by the electric field present herein (Figure 6) will allow these structures to be used as individual storage units in an electro-optical device according their wavelength and intensity.

Moreover, lanthanide ions have also attracted considerable attention for molecular magnetic information storage since their huge magnetic anisotropy permitted the observation of single-molecule magnetic (SMM) behavior.[24,25] In **DyPraNO** compounds, typical slow single-molecule magnetic relaxation with an effective energy barrier of 176.6 K was observed (Figures S9 and S10). Consequently, ITO/**DyPraNO**/Cu-(NO3)2@PEO/Pt may be the key to investigate the possibility of combined magnetic and optical information storage devices in the future.

CONCLUSION

In summary, a series of evaporable β-diketonate Ln-based dimers (**LnPraNO**) has been synthesized. Tb, Dy, and Eu derivatives exhibit luminescence upon UV irradiation that is drastically modified upon Cu^{2+} ions addition in ethanol solution. The construction of a complete solid state ITO/**LnPraNO**/Cu ions@PEO/Pt device (Ln = Eu, Tb, and Dy) makes it possible that these properties can be transferred at the solid state. In other words, we report a proof-of-concept full solid-state optoelectronic information storage unit, wherein one can write the data with an electrical stimulus, while being read through the photoluminescence output signals according to their wavelength and intensities. Additional bistability of slow single-molecule magnetic relaxation of the **DyPraNO** compounds may also provide a more flexible read/write approach to increase the information storage abilities of such systems in the future.

EXPERIMENTAL SECTION

Synthetic Procedure. All reagents were analytical grade and used as received. $Ln(hfac)_3{\cdot}2H_2O$ precursors were synthesized according to previously reported methods.[26] Pyrazine-N-oxide was purchased from TCI chemicals. $Ln(hfac)_3{\cdot}2H_2O$ (0.2 mmol) (Ln = Dy, Eu) was added to 15 mL of boiling $CHCl_3$. Then, a 10 mL dry $CHCl_3$ solution of pyrazine-N-oxide (0.2 mmol) was added drop by drop. The resulting boiling mixture was stirred for 5 min and then cooled to room temperature. After some days of slow evaporation, big pale yellow (Tb^{3+}, Dy^{3+}, Eu^{3+}) prisms were obtained. Elemental analysis calcd. (%) for $F_{36}C_{38}H_{14}Dy_2N_4O_{14}$: C, 25.94; H, 0.80; N, 3.18; Found: C, 26.13; H, 0.85; N, 3.21. calcd. (%) for $F_{36}C_{38}H_{14}Eu_2N_4O_{14}$: C, 26.23; H, 0.81; N, 3.22; Found: C, 26.32; H, 0.84; N: 3.22. calcd. (%) for $F_{36}C_{38}H_{14}Eu_2N_4O_{14}$: C, 26.02; H, 0.80; N, 3.19; Found: C, 26.24; H, 0.84; N, 3.21.

Crystal Structure Determination. A single crystal was mounted on a APEXII AXS-Bruker diffractometer equipped with a CCD camera and a graphite-monochromated Mo K radiation source (d = 0.71073 Å), from the Centre de Diffractométrie (CDFIX), Université de Rennes 1, France. Data were collected at 150 K. The structure was solved with a direct method using the SIR-97 program[27] and refined with a full-matrix least-squares method on F2 using the SHELXL-97 program[28] and WinGx interface.[29] Crystallographic data are

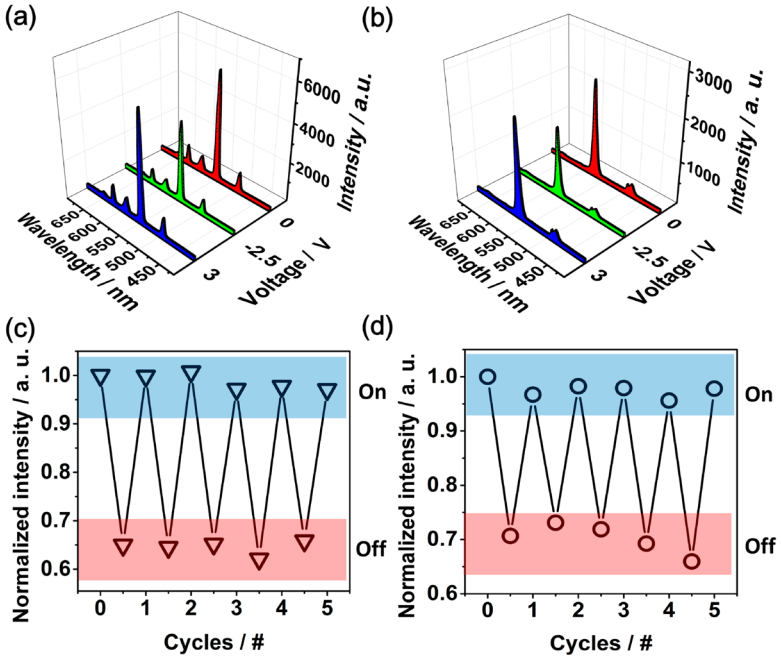

Figure 5. Photoluminescence spectra of the (a) Tb- and (b) Dy-based devices after being subjected to various electric fields. Reproducible normalized photoluminescence intensity of the (c) Tb-based device at 545 nm and (d) Dy-based device at 575 nm against alternating negative and positive electric fields. (The luminescent intensity is normalized by the initial luminescent intensity of the device at 545 and 575 nm, respectively.)

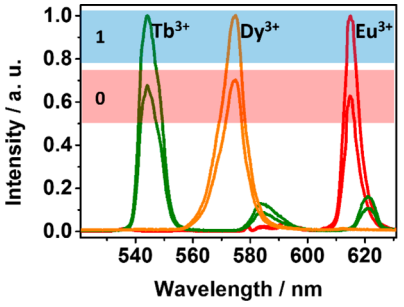

Figure 6. Illustration of electrical driven wavelength-dependent information storage based on the different luminescence states of devices made of **EuPraNO**, **TbPraNO**, and **DyPraNO**.

summarized in Table S1. CCDC-1455178 contains the supplementary crystallographic data for this paper. These data can be obtained free of charge from The Cambridge Crystallographic Data Centre via www.ccdc.cam.ac.uk/data_request/cif.

Powder X-ray Diffraction. Diagrams have been collected using a Panalytical X'Pert Pro diffractometer with an X'Celerator detector. The typical recording conditions were 45 kV and 40 mA for Cu Kα (λ = 1.542 Å); the diagrams were recorded in θ–θ mode in 6 min between 5° and 45° (8378 measurements).

Luminescence Measurements. Powder state and liquid state luminescent measurements were collected using an Horiba-JobinYvon Fluorolog III spectrofluorometer. The spectrofluorometer was beforehand calibrated using the 467 nm most intense peak of the lamp for excitation wavelength and Raman emission peak of water at 397 nm for 350 nm UV irradiation. Luminescence spectra were all recorded at room temperature in identical operating conditions without turning the lamp off to ensure a valid comparison between the emission spectra. Reproducibility of the measurements has been carefully checked. All spectra have been recorded at λ_{exc} that is found to be the maximum of the respective excitation spectra. Quantum yield measurements were performed at 293 K by evaluating the ratio of emitted photons by absorbed photons, that is

$$Q_y = (E_c - E_a)/(L_a - L_c) \quad (2)$$

where E_c is the integral of the emission spectrum of the sample, E_a is the integral of the emission spectrum of the empty sphere, L_a is the integral of the blank absorption spectrum of the empty sphere, and L_c is the integral of the absorption spectrum of the sample.

Device Fabrication. The $Cu(NO_3)_2$@PEO thin film was deposited on a commercially available Pt/SiO2/Si substrate with the spin coating method. The **LnPraNO** thin film was then deposited on the $Cu(NO_3)_2$@PEO thin film by thermal deposition. After that, the transparent conductive ITO thin film was then deposited on the previously mentioned thin films by using the pulsed laser deposition system at room temperature with the oxygen pressure varied between 0.8 and 1 Pa. The deposition frequency of ITO thin films was set to 1 Hz.

Device Structure Characterization. The crystalline structure of the as-deposited **LnPraNO** films was investigated by a grazing-incidence X-ray diffraction technique (GIXRD, Bruker AXS, D8 Discover) using Cu Kα radiation. The incidence angle of X-ray beam was fixed at 1°, and the measurements were recorded with a step of 0.05° in the range of 5° to 45°. The thickness of the films was determined using field-emission scanning electron microscopy (FESEM, Hitachi, S-4800) with 10 kV accelerating voltage.

The photoluminescent intensities of ITO/**LnPraNO**/Cu-$(NO_3)_2$PEO/Pt structures after applying various electrical fields were measured on a homemade probe station equipped with a precision semiconductor parameter analyzer (Agilent B1500) and laser confocal luminescent microscopy with Andor iR303 spectrometer. Importantly, the luminescence measurements were performed after removing the applied electrical field in order to avoid possible electroluminescence.

Magnetic dc and ac Measurements. Samples were measured on a polycrystalline state compressed tightly by Polyethylene film to avoid in-field orientation of the crystallites. Measurements were corrected for the diamagnetic contribution, as calculated with Pascal's constants, and for the diamagnetism of the sample holder, as independently determined. ac susceptibility has been measured with a Quantum Design MPMS magnetometer in the low frequency range and PPMS magnetometer in the high frequency range.

■ ASSOCIATED CONTENT

Supporting Information

The Supporting Information is available free of charge on the ACS Publications website at DOI: 10.1021/acsami.6b04451.

Additional structural, spectroscopic, and magnetic properties of the lanthanide complexes. (PDF)

■ AUTHOR INFORMATION

Corresponding Authors

*E-mail: liug@nimte.ac.cn (G.L.).
*E-mail: runweili@nimte.ac.cn (R.-W.L.).
*E-mail: kevin.bernot@insa-rennes.fr (K.B.).

Notes

The authors declare no competing financial interest.

■ ACKNOWLEDGMENTS

We thank Dr. Pravarthana Dhanapal, Ms. Wuhong Xue, and Mr. Xipao Chen for the discussion. This work was supported by the State Key Project of Fundamental Research of China (973 Program, 2012CB933004), National Natural Science Foundation of China (61504154, 11274322, 51303194, 61328402, 61306152, 11474295, 61574146, 51525103), China Postoctoral Science Foundation Funded Project (2014M560499), the Instrument Developing Project of the Chinese Academy of Sciences (YZ201327), the Youth Innovation Promotion Association of the Chinese Academy of Sciences, Ningbo Major Project for Science and Technology (2014B11011), Ningbo Science and Technology Innovation Team (2015B11001), Ningbo Natural Science Foundation (2014A610152), and Ningbo International Cooperation Projects (2014D10005).

■ REFERENCES

(1) Zimmermann, S.; Wixforth, A.; Kotthaus, J. P.; Wegscheider, W.; Bichler, M. A Semiconductor-based Photonic Memory Cell. *Science* **1999**, *283* (5406), 1292−1295.

(2) Mutai, T.; Satou, H.; Araki, K. Reproducible On-Off Switching of Solid-State Luminescence by Controlling Molecular Packing Through Heat-Mode Interconversion. *Nat. Mater.* **2005**, *4* (9), 685−687.

(3) Sagara, Y.; Kato, T. Mechanically Induced Luminescence Changes in Molecular Assemblies. *Nat. Chem.* **2009**, *1* (8), 605−610.

(4) Audebert, P.; Miomandre, F. Electrofluorochromism: from Molecular Systems to Set-Up and Display. *Chem. Sci.* **2013**, *4* (2), 575−584.

(5) Sun, H.; Liu, S.; Lin, W.; Zhang, K. Y.; Lv, W.; Huang, X.; Huo, F.; Yang, H.; Jenkins, G.; Zhao, Q.; Huang, W. Smart Responsive Phosphorescent Materials for Data Recording and Security Protection. *Nat. Commun.* **2014**, *5*, 3601−3609.

(6) Ríos, C.; Stegmaier, M.; Hosseini, P.; Wang, D.; Scherer, T.; Wright, C. D.; Bhaskaran, H.; Pernice, W. H. P. Integrated All-photonic Non-volatile Multi-level Memory. *Nat. Photonics* **2015**, *9* (11), 725−732.

(7) Kim, K.-H.; Gaba, S.; Wheeler, D.; Cruz-Albrecht, J. M.; Hussain, T.; Srinivasa, N.; Lu, W. A Functional Hybrid Memristor Crossbar-Array/CMOS System for Data Storage and Neuromorphic Applications. *Nano Lett.* **2012**, *12* (1), 389−395.

(8) Zijlstra, P.; Chon, J. W. M.; Gu, M. Five-Dimensional Optical Recording Mediated by Surface Plasmons in Gold Nanorods. *Nature* **2009**, *459* (7245), 410−413.

(9) Bünzli, J.-C.; Eliseeva, S. Basics of Lanthanide Photophysics. In *Lanthanide Luminescence*; Hänninen, P., Härmä, H., Eds.; Springer: Berlin Heidelberg, 2011; Vol. 7, pp 1−45.

(10) Di Piazza, E.; Norel, L.; Costuas, K.; Bourdolle, A.; Maury, O.; Rigaut, S. d-f Heterobimetallic Association between Ytterbium and Ruthenium Carbon-Rich Complexes: Redox Commutation of Near-IR Luminescence. *J. Am. Chem. Soc.* **2011**, *133* (16), 6174−6176.

(11) Sato, T.; Higuchi, M. An Alternately Introduced Heterometallo-Supramolecular Polymer: Synthesis and Solid-state Emission Switching by Electrochemical Redox. *Chem. Commun.* **2013**, *49* (46), 5256−5258.

(12) Tropiano, M.; Kilah, N. L.; Morten, M.; Rahman, H.; Davis, J. J.; Beer, P. D.; Faulkner, S. Reversible Luminescence Switching of A Redox-Active Ferrocene-Europium Dyad. *J. Am. Chem. Soc.* **2011**, *133* (31), 11847−11849.

(13) Tang, Q.; Liu, S.; Liu, Y.; Miao, J.; Li, S.; Zhang, L.; Shi, Z.; Zheng, Z. Cation Sensing by A Luminescent Metal-Organic Framework with Multiple Lewis Basic Sites. *Inorg. Chem.* **2013**, *52* (6), 2799−2801.

(14) Chen, B.; Wang, L.; Xiao, Y.; Fronczek, F. R.; Xue, M.; Cui, Y.; Qian, G. A Luminescent Metal-Organic Framework with Lewis Basic Pyridyl Sites for the Sensing of Metal Ions. *Angew. Chem., Int. Ed.* **2009**, *48* (3), 500−503.

(15) Hu, B.; Zhu, X.; Chen, X.; Pan, L.; Peng, S.; Wu, Y.; Shang, J.; Liu, G.; Yan, Q.; Li, R.-W. A Multilevel Memory Based on Proton-Doped Polyazomethine with An Excellent Uniformity in Resistive Switching. *J. Am. Chem. Soc.* **2012**, *134* (42), 17408−17411.

(16) Zhu, X.-J.; Shang, J.; Li, R.-W. Resistive Switching Effects in Oxide Sandwiched Structures. *Front. Mater. Sci.* **2012**, *6* (3), 183−206.

(17) Zhu, X.; Su, W.; Liu, Y.; Hu, B.; Pan, L.; Lu, W.; Zhang, J.; Li, R.-W. Observation of Conductance Quantization in Oxide-Based Resistive Switching Memory. *Adv. Mater.* **2012**, *24* (29), 3941−3946.

(18) Yi, X.; Bernot, K.; Pointillart, F.; Poneti, G.; Calvez, G.; Daiguebonne, C.; Guillou, O.; Sessoli, R. A Luminescent and Sublimable Dy-III-Based Single-Molecule Magnet. *Chem. - Eur. J.* **2012**, *18* (36), 11379−11387.

(19) Melavanki, R. M.; Kusanur, R. A.; Kulakarni, M. V.; Kadadevarmath, J. S. Role of Solvent Polarity on the Fluorescence Quenching of Newly Synthesized 7,8-benzo-4-azidomethyl Coumarin by Aniline in Benzene-acetonitrile Mixtures. *J. Lumin.* **2008**, *128* (4), 573−577.

(20) Lewandowski, A.; Stępniak, I.; Grzybkowski, W. Copper Transport Properties in Polymer Electrolytes Based on Poly(ethylene oxide) and Poly(acrylonitrile). *Solid State Ionics* **2001**, *143* (3−4), 425−432.

(21) Shang, J.; Liu, G.; Yang, H.; Zhu, X.; Chen, X.; Tan, H.; Hu, B.; Pan, L.; Xue, W.; Li, R.-W. Thermally Stable Transparent Resistive Random Access Memory based on All-Oxide Heterostructures. *Adv. Funct. Mater.* **2014**, *24* (15), 2171−2179.

(22) Binnemans, K. Chapter 225 - Rare-earth beta-diketonates. In *Handbook on the Physics and Chemistry of Rare Earths*; Karl, A., Gschneidner, J.-C. G. B., Vitalij, K. P., Eds.; Elsevier: New York, 2005; Vol. 35, pp 107−272.

(23) Du, C.; Ma, W.; Chang, T.; Sheridan, P.; Lu, W. D. Biorealistic Implementation of Synaptic Functions with Oxide Memristors through Internal Ionic Dynamics. *Adv. Funct. Mater.* **2015**, *25* (27), 4290−4299.

(24) Woodruff, D. N.; Winpenny, R. E. P.; Layfield, R. A. Lanthanide Single-Molecule Magnets. *Chem. Rev.* **2013**, *113* (7), 5110−5148.

(25) Feringa, B. L. *Molecular Switches*; Wiley-VCH Verlag GmbH: Weinheim, 2001; p 1−30.

(26) Bernot, K.; Bogani, L.; Caneschi, A.; Gatteschi, D.; Sessoli, R. A Family of Rare-Earth-Based Single Chain Magnets: Playing with Anisotropy. *J. Am. Chem. Soc.* **2006**, *128* (24), 7947−7956.

(27) Altomare, A.; Burla, M. C.; Camalli, M.; Cascarano, G. L.; Giacovazzo, C.; Guagliardi, A.; Moliterni, A. G. G.; Polidori, G.; Spagna, R. SIR97: A New Tool for Crystal Structure Determination and Refinement. *J. Appl. Crystallogr.* **1999**, *32*, 115−119.

(28) Sheldrick, G. M.; Schneider, T. R. SHELXL: High-Resolution Refinement. *Methods Enzymol.* **1997**, *277*, 319−343.

(29) Farrugia, L. J. WinGX Suite for Small-Molecule Single-Crystal Crystallography. *J. Appl. Crystallogr.* **1999**, *32*, 837−838.